ADA013106

THIRD QUARTER FY75 APPLIED OPTICS RESEARCH REPORT

by

Staff of the Optical Sciences Center
University of Arizona
Dr. P. A. Franken, Director

May 1975

Prepared for the
Space and Missile Systems Organization
Air Force Systems Command
Los Angeles Air Force Station, California
Under contract FO 4695-67-C-0197

Optical Sciences Center
University of Arizona
Tucson, Arizona 85721

AVAILABILITY NOTICE

Approved for public release; distribution unlimited.

DISPOSITION INSTRUCTIONS

Do not return this copy. Retain or destroy.

REPRODUCTION NOTICE

This report may be reproduced for any purpose of
the U.S. Government.

SECURITY CLASSIFICATION OF THIS PAGE (When Data Entered)
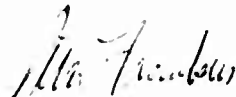
REPORT DOCUMENTATION PAGE		READ INSTRUCTIONS BEFORE COMPLETING FORM
1. REPORT NUMBER SAMSO TR 75-152	2. GOVT ACCESSION NO.	3. RECIPIENT'S CATALOG NUMBER
4. TITLE (and Subtitle) APPLIED OPTICS RESEARCH REPORT		5. TYPE OF REPORT & PERIOD COVERED Quarterly report, no. 3 1 Jan – 31 Mar 1975
		6. PERFORMING ORG. REPORT NUMBER
7. AUTHOR(s) Optical Sciences Center Technical Staff P. A. Franken, Director		8. CONTRACT OR GRANT NUMBER(s) FO 4695-67-C-0197
9. PERFORMING ORGANIZATION NAME AND ADDRESS Optical Sciences Center University of Arizona Tucson, Arizona 85721		10. PROGRAM ELEMENT, PROJECT, TASK AREA & WORK UNIT NUMBERS 58 p.
11. CONTROLLING OFFICE NAME AND ADDRESS SAMSO/DYS Los Angeles Air Force Station, California		12. REPORT DATE May 1975
		13. NUMBER OF PAGES 54
14. MONITORING AGENCY NAME & ADDRESS(if different from Controlling Office) HQ SAMSO/DYS P.O. Box 92960, Worldway Postal Center Los Angeles, California 90009		15. SECURITY CLASS. (of this report) Unclassified
		15a. DECLASSIFICATION/DOWNGRADING SCHEDULE

16. DISTRIBUTION STATEMENT (of this Report)

Approved for public release; distribution unlimited

17. DISTRIBUTION STATEMENT (of the abstract entered in Block 20, if different from Report)

18. SUPPLEMENTARY NOTES

19. KEY WORDS (Continue on reverse side if necessary and identify by block number)

Image processing
Mathematical optics
Optical tracking
Quantum optics

20. ABSTRACT (Continue on reverse side if necessary and identify by block number)

This third quarter FY75 status report of the University of Arizona Optical Sciences Center presents results of work in program areas supported entirely or in part by USAF Contract FO-4695-67-C-0197. Specifically covered in this report are image processing, mathematical optics, optical tracking, and quantum optics. Also included is a list of professional publications and activities of Optical Sciences Center personnel.

DD FORM 1473 1 JAN 73   EDITION OF 1 NOV 65 IS OBSOLETE
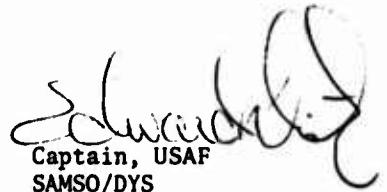
UNCLASSIFIED

FOREWORD

This status report of the Optical Sciences Center, University of Arizona, Tucson, Arizona, under U.S. Air Force Contract FO-4695-67-C-0197, covers research progress for the period 1 January 1975 to 31 March 1975.

This contract was issued by the Department of the Air Force, Space and Missile Systems Organization (AFSC), P.O. Box 92960, Worldway Postal Center, Los Angeles, California 90009, and is administered by the ONRRR, University of Arizona, Tucson, Arizona 85721.

The use of trade names in this report does not constitute an official endorsement or approval of the use of such commercial hardware or software. This report may not be cited for purposes of advertisement, and its publication does not constitute Air Force approval of findings or conclusions.

Director
Optical Sciences Center

Captain, USAF
SAMSO/DYS

CONTENTS

PROFESSIONAL PUBLICATIONS AND ACTIVITIES

OF OPTICAL SCIENCES CENTER PERSONNEL

(listed chronologically)

Journal Publications

George Lamb, Jr., "Bäcklund transformation for certain nonlinear evolution equations," J. Math Phys. 15(12):2157-2165, Dec. 1974 (publication not received until this quarter).

D. Rogovin and *Marlan O. Scully*, "Does the 'two-level atom' picture of a Josephson junction have a theoretical foundation in BCS?" Ann. Phys. 88(2):371-396, Dec. 1974 (publication not received until this quarter).

R. L. Shoemaker, S. Stenholm, and Richard G. Brewer, "Collision-induced optical double resonance," Phys. Rev. 10(6):2037-2050, Dec. 1974 (publication not received until this quarter).

S. F. Jacobs, M. Sargent III, J. F. Scott, and *M. O. Scully*, eds., *The Physics of Quantum Electronics, Vol. II, Laser Applications to Optics and Spectroscopy*, Addison-Wesley, Reading, Mass., 1974 (publication not received until this quarter).

Peter H. Bartels, George B. Olson, Jack M. Layton, Robert E. Anderson, and George L. Wied, "Computer discrimination of T and B lymphocytes," Acta Cytologica 19(1):53-57, Jan.-Feb. 1975.

R. E. Anderson, G. B. Olson, C. Shank, T. L. Howarth, G. L. Wied, and *P. H. Bartels*, "Computer analysis of defined populations of lymphocytes irradiated in vitro. I. Evaluation of murine thoracic duct lymphocytes," Acta Cytologica 19(1):126-135, Jan.-Feb. 1975.

W. M. Fairbank, Jr., G. K. Klauminzer, and A. L. Schawlow, "Excited-state absorption in ruby, emerald, and $MgO:Cr^{3+}$," Phys. Rev. B11:60-76, Jan. 1975.

V. N. Mahajan and *J. D. Gaskill*, "Diffraction of light by sound waves in optically isotropic media," Opt. Eng. 14:91-97, Jan.-Feb. 1975.

A. S. Marathay, "Polarized light and its application, I," Opt. Eng. 14:S-17 to S-21, Jan.-Feb. 1975.

M. P. Rimmer and *J. C. Wyant*, "Evaluation of large aberrations using a lateral-shear interferometer having variable shear," Appl. Opt. 14:142-150, Jan. 1975.

W. M. Fairbank, Jr., T. W. Hänsch, and A. L. Schawlow, "Absolute measurement of very low sodium-vapor densities using laser resonance fluorescence," J. Opt. Soc. Am. 65(2):199-204, Feb. 1975.

J. B. Hambenne and *M. Sargent III*, "Physical interpretation of bistable unidirectional ring-laser operation," IEEE J. Quantum Electronics QE-11:90-92, Feb. 1975.

D. Rogovin, H. Tigalaar, and *M. Sargent III*, "A simple, reliable model of the bending mode of water," Chem. Phys. Letters 31:147-153, Feb. 1975.

H. Shih, M. O. Scully, P. V. Avizonis, and W. H. Louisell, "Multimode approach to the physics of unstable laser resonators," Phys. Rev. A11:630-647, Feb. 1975.

O. N. Stavroudis, Book review of *Optics* by E. Hecht and A. Zajac, Addison-Wesley, Reading, Mass., 1974; Phys. Today 28(2):54-55, Feb. 1975.

F. O. Bartell and *W. L. Wolfe*, "New approach for the design of blackbody simulators," Appl. Opt. 14(2):249-252, Feb. 1975.

R. A. Johnston and *C. L. Babcock*, "Composition dependence of elastic moduli in $Na_2O-TiO_2-SiO_2$ glasses," J. Am. Ceram. Soc. 58(3-4): 85-87, Mar.-Apr. 1975.

V. N. Mahajan, "Real-time wavefront correction through Bragg diffraction of light by sound waves," J. Opt. Soc. Am. 65(3):271-278, Mar. 1975.

D. Rogovin, "Electrodynamics of Josephson junctions," Phys. Rev. B11(5): 1906-1908, Mar. 1975.

M. H. Farmelant, C. D. DeMeester, D. T. Wilson, and *H. H. Barrett*, "Initial clinical experiences with a Fresnel zone plate imager," J. Nucl. Med. 16:183-187, 1975.

D. Rogovin, "Phase coherence in two-band superconductors," J. Low Temp. Phys. 18($\frac{1}{2}$):1-2, 1975.

Invited Papers

B. R. Frieden, "Super-resolution, entropy and phase contrast," at a special seminar of the National Radio Astron. Observ., Charlottesville, Virginia, Jan. 13, 1975.

B. O. Seraphin, "Solar utilization now short course (SUN) on solar energy," Arizona State University, Tempe, Arizona, Jan. 13-14, 1975.

M. O. Scully, "Charge exchange excitation--x-ray laser," Orbis Scientiae II, Center for Theoretical Studies, University of Miami, Coral Gables, Florida, Jan. 19-24, 1975.

M. O. Scully, "Resonant charge exchange," Orbis Scientiae II, Center for Theoretical Studies, University of Miami, Coral Gables, Florida, Jan. 19-24, 1975.

B. O. Seraphin, "Spectrally selective surfaces for high temperature photo thermal conversion," 1975 Joint Meeting of the American Physical Society and the American Association of Physics Teachers, Anaheim, California, Jan. 29-Feb. 1, 1975.

M. O. Scully, "Resonant charge exchange," and "Short λ and superradiant resonators," 5th Winter Colloquium on Quantum Electronics, Snowmass, Colorado, Feb. 1-6, 1975.

W. Swindell, L. R. Doose, M. Tomasko, and J. Fountain, "The Pioneer 11 images of Jupiter," presented at the 6th Annual Meeting of the Division for Planetary Sciences, American Astronomical Society, Feb. 17-21, 1975.

4

Conference Proceedings

H. H. Barrett, "Fresnel zone plate and related coded apertures," in *Proceedings of the SPIE National Seminar on Coherent Optical Processing, Vol. 52,* H. J. Caulfield, ed. (Meeting held August 21-22, 1974, San Diego, California).

R. Buchroeder, "Tilted component optical design methods for infrared," in *Proceedings of the SPIE National Seminar on Applications of Geometrical Optics, Vol. 39,* Warren J. Smith, ed. (Meeting held August 27-29, 1973, San Diego, California).

James J. Burke, "Estimating objects from their blurred and grainy images," in *Proceedings of the Technical Program, Electro-Optical Systems Design Conference-1974 West, International Laser Exposition* (Meeting held November 5-7, 1974, San Francisco, California).

A. B. Meinel, "Optical interfaces in solar energy utilization," in *Proceedings of the SPIE National Seminar on Effective Systems Integration & Optical Design, Vol. 54,* G. Wilkerson and R. W. Poindexter, eds. (Meeting held August 21-23, 1974, San Diego, California).

M. Ruda, "Optical tolerancing for multi-mirror telescope," in *Proceedings of the SPIE National Seminar on Applications of Geometrical Optics, Vol. 39,* Warren J. Smith, ed. (Meeting held August 27-29, 1973, San Diego, California).

R. A. Schowengerdt, "Measurement of earth resources technology satellite (ERTS-1) multispectral scanner OTF from operational imagery," in *Proceedings of the SPIE/OSA National Seminar on Image Assessment & Specification, Vol. 46,* D. Dutton, ed. (Meeting held May 20-22, 1974, Rochester, New York).

R. V. Shack, "Significance of phase transfer function," in *Proceedings of the SPIE/OSA National Seminar on Image Assessment & Specification, Vol. 46,* D. Dutton, ed. (Meeting held May 20-22, 1974, Rochester, New York).

R. V. Shack, "Use of normalization in application of simple optical systems," in *Proceedings of the SPIE National Seminar on Effective Systems Integration & Optical Design, Vol. 54,* G. Wilkerson and R. W. Poindexter, eds. (Meeting held August 21-23, 1974, San Diego, California).

R. V. Shack, "Analytic system design with pencil & ruler--advantages of y-ȳ diagram," in *Proceedings of the SPIE National Seminar on Applications of Geometrical Optics, Vol. 39,* Warren J. Smith, ed. (Meeting held August 27-29, 1973, San Diego, California).

R. R. Shannon, "Fringe benefits in testing," in *Proceedings of the SPIE National Seminar on Applications of Geometrical Optics, Vol. 39,* Warren J. Smith, ed. (Meeting held August 27-29, 1973, San Diego, California).

R. R. Shannon, "Massive optical technology at the Optical Sciences Center," in *Proceedings of the Technical Program, Electro-Optical Systems Design Conference-1974 West, International Laser Exposition* (Meeting held November 5-7, 1974, San Francisco, California).

Philip N. Slater and William L. Wolfe, eds., *Proceedings of the SPIE National Seminar on Scanners & Imagery Systems for Earth Observation, Vol. 51,* (Meeting held August 19-20, 1974, San Diego, California).

P. N. Slater, "Specifications for remote sensing photographic systems," in *Proceedings of the SPIE National Seminar on Effective Systems Integration & Optical Design, Vol. 54,* G. Wilkerson and R. W. Poindexter, eds. (Meeting held August 21-23, 1974, San Diego, California).

James M. Palmer and William L. Wolfe, "The optics and calibration of the Venus solar flux radiometer," in *Proceedings of the Technical Program, Electro-Optical Systems Design Conference-1974 West, International Laser Exposition* (Meeting held November 5-7, 1974, San Francisco, California).

Frederick O. Bartell and William L. Wolfe, "A comparison of the performance of blackbody simulators of different shapes," in *Proceedings of the Technical Program, Electro-Optical Systems Design Conference-1974 West, International Laser Exposition* (Meeting held November 5-7, 1974, San Francisco, California).

Contributed Papers

R. E. Hahn and B. O. Seraphin, "Thick semiconductor films for photo-thermal solar energy conversion," Conference on Structure Property Relationships in Thick Film and Bulk Coatings, San Francisco, California, Feb. 10-12, 1975.

J. Hambenne and M. Sargent III, "Physical interpretation of bistable, unidirectional ring laser operation," Bull. Am. Phys. Soc., Anaheim, California, 1975.

Technical Reports and Government Reports

B. O. Seraphin, "Chemical vapor deposition research for fabrication of solar energy convertors," NSF/RANN 1974 Annual progress report, Grant No. GI-36731X.

R. A. Schowengerdt and P. N. Slater, "Evaluation of ERTS-1 image sensor spatial resolution in photographic form," NASA/Goddard Space Flight Center, Jan. 1975.

P. A. Franken, "Semi-annual FY75 applied optics research report," SAMSO TR 75-112, January 1975.

R. R. Shannon, R. V. Shack, T. R. Gurski, D. W. Hillman, F. A. Hopf, R. L. Shoemaker, I. R. Harrison, and J. C. Wyant, "Optical tracking system study interim report," Space and Missile Test Center, FO-4703-75-C-0210, February 1975.

P. H. Bartels, J. J. Burke, B. R. Frieden, R. S. Hershel, and L. Wheeler, "Basic and applied research in optical science and technology," annual report on F-33657-C-605, February, 1975.

Colloquia

D. N. Rogovin, "Molecular spectroscopy," Kirtland AFB, January 8-9, 1975.

M. Sargent III, "Multimode model of water molecule," Kirtland AFB, January 8-9, 1975.

G. Lamb, Jr., "Coherent optical pulse propagation," Applied Mathematics Seminar, California Institute of Technology, January 20, 1975.

B. R. Frieden, "Super-resolution by Fresnel-encoding the image," Optical Sciences Center Colloquium, January 30, 1975.

H. H. Barrett, "Coded aperture imaging," Biomedical Engineering Seminar, University of Arizona, February 3, 1975.

R. L. Shoemaker, "Infrared quantum beat spectroscopy," Physics Dept., University of Arizona, February 18, 1975.

J. D. Gaskill, "The status and future of holography," Optical Sciences Center Colloquium, February 20, 1975.

M. O. Scully, invited lectures at Physics Dept., University of Colorado and Joint Institute for Laboratory Astrophysics, Feb. 24-28, 1975.

M. Meinel, "Solar energy," University of Wisconsin, Milwaukee, Wisconsin, March 5, 1975.

W. Fairbank, "Detection of small quantities of matter by laser resonance fluorescence," Colorado State University, March 11, 1975.

J. M. Palmer and M. G. Tomasko, "The 1978 Pioneer-Venus solar flux experiment," University of Arizona Atmospheric Sciences Colloquium, March 14, 1975.

A. B. Meinel and M. Meinel, "Solar energy," Weber State College, Ogden, Utah, March 27, 1975.

L. Wheeler, "Review of psychophysical investigations of image quality," SAMSO, Los Angeles, California, March 12, 1975.

Organization of Scientific Meetings and Courses

P. A. Franken, Chairman, "Committee on Society Objectives and Policy (SOAP) of the Optical Society of America," Tucson, Arizona Jan. 10-11, 1975.

M. O. Scully, Session moderator, "X-ray laser session, Orbis Scientiae II," at Center for Theoretical Studies, University of Miami, Coral Gables, Florida, Jan. 19-24, 1975.

B. O. Seraphin, organized session on "Physics of solar energy conversion," at American Physical Society meeting, Anaheim, California, Jan. 29-Feb. 1, 1975.

M. O. Scully, Co-director, "5th Winter Colloquium on Quantum Electronics," Snowmass, Colorado, Feb. 1-6, 1975.

B. O. Seraphin, organized planning session of the "National Science Foundation's Workshop on Material Sciences," at Harvard University, Cambridge, Massachusetts, Feb. 13-17, 1975.

R. V. Shack, "Optical Fabrication & Testing Workshop," sponsored by the Optical Society of America, San Francisco, California, Mar. 13-16 and Anaheim, California, Mar. 19-21, 1975.

R. R. Shannon, Chairman, Panel discussion on "Applications of Laser Spectroscopy," at Optical Society of America meeting, Anaheim, California, March 20, 1975.

New Committee Memberships

P. A. Franken, Ballistic Missile Defense Technology Advisory Panel, Department of the Army, Huntsville, Alabama.

M. Sargent III, U.S. Senior Scientist Award, fellowship for pursuit of research in Germany.

B. O. Seraphin, participant in joint USSR - USA workshop on Solar Central Power Stations, Colorado State University, Ft. Collins, Colorado, March 30-April 1, 1975.

B. O. Seraphin, Consultant to NASA - Marshall Space Flight Center on recommendations for the implementation of the Solar Heating & Cooling Act being put together, March 1975.

L. Wheeler, Acting Chairman, Department of Psychology, University of Arizona, January 1, 1975.

W. L. Wolfe, American Editor of Infrared Physics.

W. L. Wolfe, Chairman of Optical Society of America Technical Group on Radiometry.

J. C. Wyant, Guest editor of Sept.-Oct. issue of Optical Engineering, organizing the special issue on "Application of Holography."

Public Service Speaking

W. Swindell, "Pioneer 10 and 11--first pictures from Jupiter," Optical
    Sciences Center Public Evening, Jan. 13, 1975.

B. O. Seraphin, "Spectrally selective coatings for solar energy con-
    version," Tucson Section Optical Society of America, January 27, 1975.

B. O. Seraphin, participat 1 in a press conference on "Solar energy
    conversion," Anaheim, California, January 30, 1975.

R. V. Shack, "Generalized performance characteristics of simple optical
    systems," Local section of the Optical Society of America, Los
    Angeles, California, February 5, 1975.

W. L. Wolfe, "Infrared techniques in diagnostic medicine," Optical
    Sciences Center Public Evening, February 10, 1975.

W. L. Wolfe, "What is Light?" Jacob E. Fruehtlendler Elementary School,
    February 11, 1975.

D. N. Rogovin, "Superconductivity and macroscopic quantum phenomena,"
    Quantum Optics and Atomic Physics Seminar, February 14, 1975.

R. R. Shannon, "Lasers," Townsend Jr. High School, February 26, 1975.

L. Wheeler, "Applications of environmental psychology to local problems,"
    Behavior Associates, Tucson, Arizona, March 4, 1975.

H. H. Barrett, "Moiré for fun and profit," Optical Sciences Center
    Public Evening, March 10, 1975.

P. A. Franken, "Things we could not say at luncheons before now,"
    University of Arizona Foundation Luncheon, Arizona Ballroom, March
    11, 1975.

R. E. Hahn, "One approach to solar energy," Program on energy, Tucson
    League of Women Voters, Tucson, Arizona, March 14, 1975.

O. N. Stavroudis, "Sir Ike and the zodiac," Brown bag seminar, March
    19, 1975.

F. Hopf, "Amplification in swept-gain systems," Quantum Optics and
    Atomic Physics Seminar, March 21, 1975.

12

L. Ralph Baker, "Pioneer/Jupiter real-time image display system,"
    Bay area chapter SMPTE, Redwood City, California, March 25, 1975.

RESEARCH ACTIVITIES

IMAGE PROCESSING

Digital Processing of Annular Coded-Aperture Imagery
(R. G. Simpson, H. H. Barrett, and H. D. Fisher)

Summary

In the past, annular coded-aperture images have been reconstructed by correlating the annulus with the coded image. The basic improvement suggested in this report is the addition of a linear radial frequency weighting in the Fourier plane. Reconstruction of point and disk objects was simulated with a computer program. The results show the advantage of this modification in the processing scheme. When the assumption is made that the detector is an Anger camera, the resolution obtained with the improved processing of the coded image is equal to that obtained with conventional apertures.

The annulus is intermediate between the pinhole and the Fresnel zone plate with regard to both collection efficiency and the number of counts required for a given signal-to-noise ratio (SNR). It therefore offers an improvement over pinhole apertures without demanding the increased count rate and resolution required of detectors when Fresnel zone plate coded apertures are used.

Introduction

. The imaging problem encountered in nuclear medicine is the formation of a picture of the distribution of radiopharmaceuticals within a patient. Isotopes commonly used in nuclear medicine emit gamma rays with energy in the 100 to 400 keV range. For photons in this energy range, reflection, refraction, and diffraction effects are so small that they are practically useless for imaging purposes. The only alternative is to use the absorption of gamma rays by matter to cast shadows.

One simple shadow-casting device is the pinhole. Another is the collimator, which restricts the field of view of a given section of the detector to a given region of the object. When either of these apertures is used, a compromise must be made between collection efficiency and resolution; as one improves, the other necessarily degrades.

Coded apertures of various descriptions have been proposed as alternatives to the pinhole and the collimator. While coded apertures collect far more counts than conventional apertures, they also require more counts to obtain the same SNR. One measure of a potential coded aperture is whether the increase in collected counts exceeds the required increase in counts for a constant SNR. In general, there will be a net advantage to coded apertures for relatively small objects, but the advantage will disappear as the object size approaches the full field of view.

One class of coded apertures, referred to as filled apertures, is roughly 50% transparent to the gamma rays. The Fresnel zone plate and Dicke's random pinhole array are examples of this type of aperture. Another class of coded apertures, called dilute apertures, is much less than 50% transparent. The nonredundant pinhole array is one example of this class. Another is the annulus that will be described here. Dilute apertures are intermediate between the filled apertures and the pinhole with regard to both collection efficiency and the number of counts needed for a given SNR.

One additional feature of coded apertures is their tomographic capability. This refers to the fact that different planes in the image can be brought into focus separately. The scale of a shadow created by an object point will depend on the distance of the object from the plane of the aperture. In this way depth information is stored in the coded image.

While this tomographic capability is a useful property, it causes some difficulty. Reconstruction usually involves correlation of the coded image with a processing function. The scale of the processing function is chosen so that a certain plane in the image will be cor-

rectly reconstructed. However, shadows with many different scales are
present in the coded image. Contributions to the reconstruction due to
these other shadows must not add structure to the image that might
result in a faulty diagnosis. Effects due to shadows with the incorrect
scale will be referred to as out-of-focus behavior.

The Annulus

The annulus consists of a sheet of absorbing material such as
lead with a circular ring cut out of it. The shadow created by such
an aperture will be described by an inner radius r_1 and an outer
radius r_2.

Walton first used the annulus as a coded aperture in nuclear
medicine.[1] Other investigators have taken an interest in it since
then.[2,3] Walton's reconstruction process was effectively a correlation
of the coded image with a thin annulus. The point spread function (PSF)
associated with such an encoding-reconstruction scheme is shown in Fig. 1.
The undesirable feature of this function is its rather long tail. Object
points are then capable of influencing the reconstruction at points
rather far from their actual positions. For this reason it is desirable
to have the PSF as compact as possible. One way to make the annular
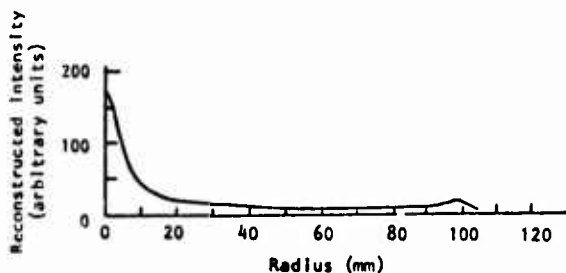aperture PSF more compact will now be discussed.

Fig. 1. Point spread function corresponding
to the autocorrelation of the annulus.

If one approximates the annulus by a ring delta function, $\delta(r - R)$, the autocorrelation has the form[4]

$$\delta(r - R) \,**\, \delta(r - R) \;=\; \frac{4R^2}{r(4R^2 - r^2)^{\frac{1}{2}}} \, . \tag{1}$$

(The double star notation indicates a two-dimensional correlation operation.) Away from the singularity at $r = 2R$, the function behaves as $1/r$. It is this behavior that needs to be eliminated. A trip to the frequency domain provides the key to this problem.

The Fourier transform of a thin annulus is closely approximated by $2\pi\bar{r}J_0(2\pi\bar{r}\rho)$ where $\bar{r} = (r_1 + r_2)/2$ and ρ is the magnitude of the spatial frequency vector in cycles (or line pairs) per unit length. To a good approximation, beyond the first zero,

$$2\pi\bar{r}J_0(2\pi\bar{r}\rho) \;\simeq\; 2(\bar{r}/\rho)^{\frac{1}{2}} \cos(2\pi\bar{r}\rho - \pi/4). \tag{2}$$

The Fourier transform of the autocorrelation of a thin annulus is then

$$\begin{aligned}
4\pi^2\bar{r}^2 J_0{}^2(2\pi\bar{r}\rho) \;&\simeq\; \frac{4\bar{r}}{\rho}\cos^2(2\pi\bar{r}\rho - \pi/4) \\[2mm]
&=\; \frac{2\bar{r}}{\rho}[1 + \cos(4\pi\bar{r}\rho - \pi/2)] \\[2mm]
&=\; \frac{2\bar{r}}{\rho}[1 + \sin 4\pi\bar{r}\rho].
\end{aligned} \tag{3}$$

If all the frequency components are weighted by ρ, the frequency spectrum becomes $2\bar{r}[1 + \sin 4\pi\bar{r}\rho]$. The constant term in frequency space will result in a spatial function sharply peaked about the origin. The sine term will contribute to the spatial function for values of r near $2\bar{r}$. That the $1/r$ behavior of the PSF can be eliminated in this way is not surprising when one recalls that[5]

$$F\{1/r\} \;=\; 1/\rho. \tag{4}$$

This use of a linear frequency weighting also occurs in the literature on computerized axial tomography where it is called a rho-filter.

It is important to realize that this linear weighting of frequencies cannot go on indefinitely. Noise considerations require a termination of this boosting. The modulation transfer function (MTF) of the detector could be used to damp the linear weighting at high spatial frequencies. Alternatively, an artificial apodization function $F(\rho)$ could be included in the frequency domain processing.

Computer Simulations

The effect of the rho-filter has been investigated with the use of a computer program that performs Fourier transforms of circularly symmetric functions. The coded image $g(\vec{r})$ is given by the convolution of the object $o(\vec{r})$ with the annulus $\text{ann}(\vec{r})$

$$g(\vec{r}) = o(\vec{r}) ** \text{ann}(\vec{r}). \tag{5}$$

(Scale factors, as discussed in Ref. 6, have been suppressed in this equation.) The coded image is Fourier transformed yielding, for circularly symmetric functions,

$$G(\rho) = O(\rho) \cdot \text{ANN}(\rho). \tag{6}$$

This function is then multiplied by the transform of a thin annulus, $2\pi\bar{r}J_0(2\pi\bar{r}\rho)$, the rho-filter, and the apodization function $F(\rho)$

$$G'(\rho) = O(\rho) \cdot \text{ANN}(\rho) \cdot 2\pi\bar{r}J_0(2\pi\bar{r}\rho) \cdot \rho \cdot F(\rho). \tag{7}$$

Then $G'(\rho)$ is inverse transformed to give the reconstructed object $g'(r)$.

For all studies reported here, the dimensions of the annular shadow in the detector plane were $r_1 = 47.5$ mm and $r_2 = 52.5$ mm. The PSF with an apodization $F(\rho)$ described by

$$F(\rho) \quad = \quad \begin{cases} 1 \text{ for } 0 \leq \rho \leq 0.125 \text{ lp/mm} \\ 0 \text{ for } \rho > 0.125 \text{ lp/mm} \end{cases} \tag{8}$$

is shown in Fig. 2a. The $1/r$ tail of Fig.1 has been eliminated. The ringing is due to the sharp cutoff in the frequency plane.

A gaussian apodization that approximates the MTF of an Anger camera with 8-mm resolution was used in Fig. 2b. The ringing has been virtually eliminated. However, the bipolar wiggle at $r = 2\bar{r}$ due to the $\sin 4\pi\bar{r}\rho$ term in Eq. (3) is still present. Except for the wiggle, the PSF is now much more compact and even has a resolution as good as that of the camera.
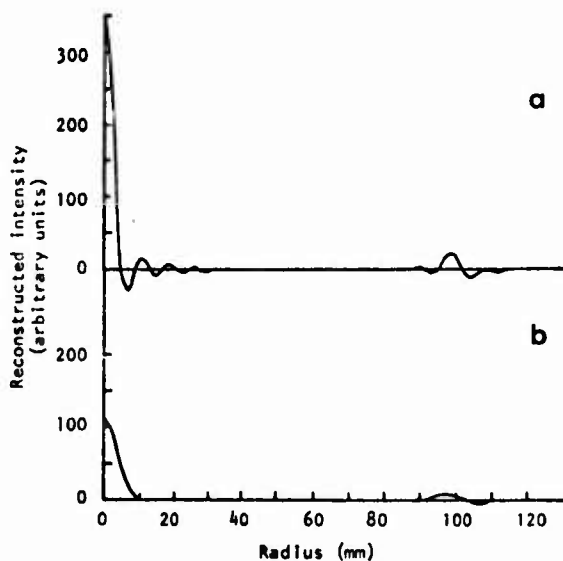
Fig. 2. Point spread function obtained with the rho-filter included. (a) Sharp cutoff in frequency plane. (b) Gaussian apodization in frequency plane.

The improvement afforded by the rho-filter operation is shown remarkably when disk objects are imaged. Figure 3 shows the reconstruction

obtained if the rho-filter operation is omitted. The vertical scale is in arbitrary units but is the same for each of the disks. The magnitude at the center depends linearly on the radius of the disk. The effect of the rho-filter is shown in Fig. 4. The magnitudes at the centers of the disks are now all the same. The true edge of each disk occurs remarkably close to the half-peak value of the reconstruction. The data beyond $r = 50$ mm are due to the bipolar wiggle of the PSF.
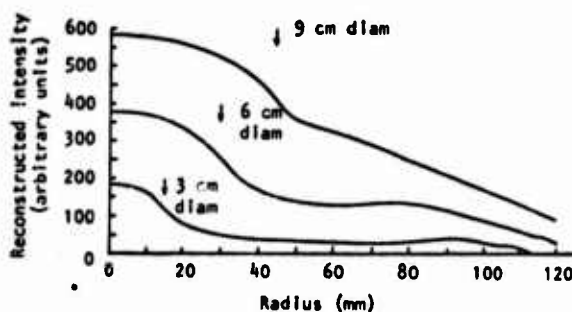

Fig. 3. Reconstruction of disk objects of several sizes by correlation with an annulus without the rho-filter operation.
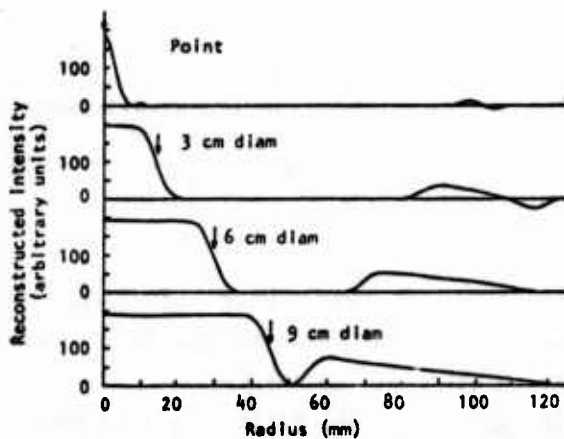

Fig. 4. Reconstruction of disk objects of several sizes by correlation with an annulus with the rho-filter operation.

Again, assuming a gaussian model for the Anger camera MTF, the reconstruction of three sets of concentric annuli was simulated with the results shown in Fig. 5. The radius of the central disk was chosen to be three quarters the width of the rings so that a well defined radial frequency would result. Three quarters was chosen because the first zero of the J_0 function occurs at approximately three quarters of the distance between consecutive zeros of the J_0 function. In Fig. 5c, the rings are slightly narrower than the resolution. The reconstruction shown in Fig. 5d still has a contrast of 35%. For the 5-mm-wide rings shown in Fig. 5e, the contrast in the reconstruction is only 10%.
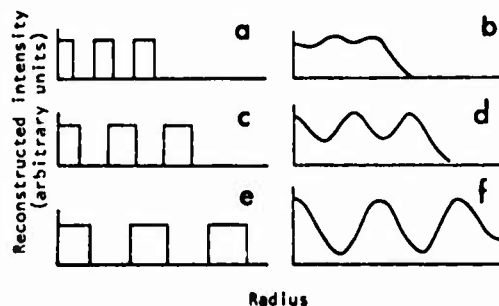
Fig. 5. Concentric ring objects and their reconstruction. The rho-filter is included along with the gaussian MTF of the Anger camera. The field of view has been limited so that artifacts due to the wiggle at $2\bar{r}$ are outside the field. (a) Object with 5-mm ring width. (b) Reconstruction of (a). (c) Object with 7-mm ring width. (d) Reconstruction of (c). (e) Object with 10-mm ring width. (f) Reconstruction of (e).

As mentioned earlier, for the tomographic capabilities of the coded-aperture reconstruction technique to be useful, the out-of-focus response should not cause confusing structure to appear. A parameter called FOCUS, defined as the ratio of the reconstructing annular radius to the coding annular radius, was investigated for its effects on the PSF. The results are shown in Fig. 6. The effect of FOCUS on the reconstruction

FOCUS = 1

FOCUS = 0.95

FOCUS = 0.9

FOCUS = 0.85

FOCUS = 0.8

0   20   40   60   80   100 120
(Radius (mm))

Reconstructed Intensity (arbitrary units)
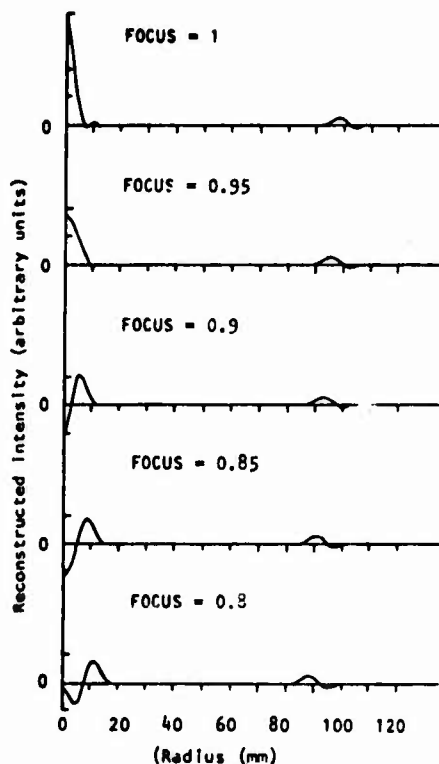
Fig. 6.   Effects of FOCUS on PSF.

of a disk object is illustrated in Fig. 7. At the present time there is no hard and fast criterion for judging the out-of-focus behavior of a coded aperture. These results do not appear disturbing, but at the same time they are not ideal.

Signal-to-Noise Ratio

When a coded aperture is used to image a point source, more counts are collected than for a pinhole. The SNR is therefore better for the coded aperture case. However, when more than one point is being imaged, the shadows created by the object points may overlap. Then counts due to one object point will be a noise source for another object point. The effects of this noise will decrease the advantage enjoyed by coded apertures.[7]

The magnitude of this decrease depends on the amount of overlap. Consider a Fresnel zone plate with the same resolution as the annulus described above. When the object consists of two points whose shadows are displaced with respect to each other by half the maximum radius of the zone plate, the overlap is roughly 40% of the open area. For the annulus under the same conditions, the overlap is only 10% of the open area. The SNR for the zone plate is therefore degraded more than for the annulus, but the zone plate has the higher geometric collection efficiency.
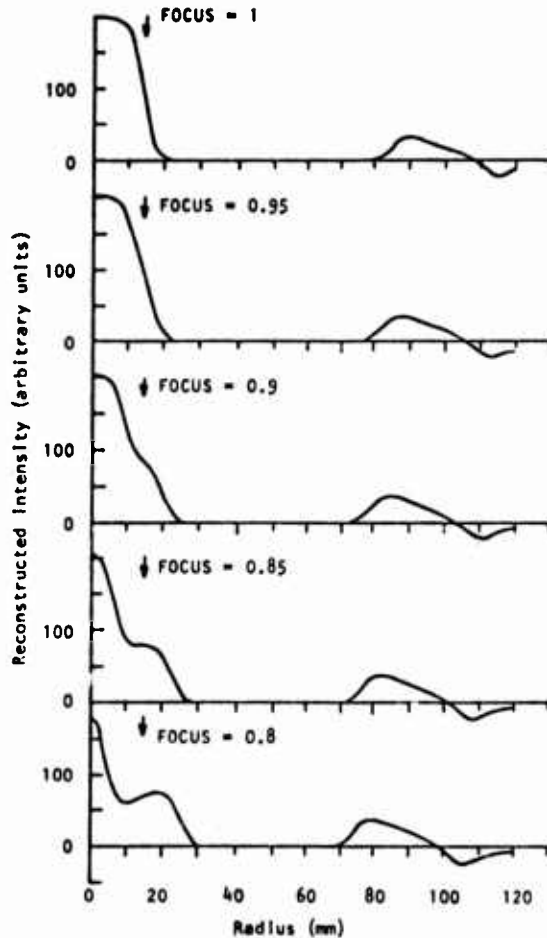
Fig. 7. Effects of FOCUS on the reconstruction of a
15-mm-radius disk.

The two factors work in opposition to one another, suggesting that the
annulus is a good alternative to the zone plate for intermediate values
of the ratio of object area to resolution cell size.

An exact comparison of the SNR characteristics of the annulus
with other coded apertures requires the calculation of the noise kernel.
A computer program is being written to provide this information. The
value of the annulus as a coded aperture will ultimately depend on this
comparison.

Detector Requirements

A short note needs to be made here regarding an advantage of the annulus over the Fresnel zone plate when an Anger camera is used as the detector. As discussed above, the annulus collects fewer counts than the Fresnel zone plate but also needs fewer for the same SNR. Therefore, the count rate capability of the camera is not taxed. In addition, the required resolution is not as great as when an off-axis Fresnel zone plate is used. Therefore, camera limitations are not as severe for the annulus as for the zone plate.

Conclusions

The improvement in the PSF provided by the rho-filter operation, along with the striking results in the disk object reconstruction, make the annulus an attractive aperture. The annulus appears well suited for the Anger camera, and resolution as good as that of the camera is attainable. Finally, on empirical grounds, the annulus shows promise of being as good as the zone plate for values of object area/ resolution cell size commonly encountered in nuclear medicine.

Acknowledgment

References

1. P. W. Walton, J. Nucl. Med. 14, 861 (1973).
2. H. H. Barrett, W. W. Stoner, D. T. Wilson, and G. D. DeMeester, Opt. Eng. 13, 539 (1974).
3. W. Ashburn, private communication.

24

4. A. Papoulis, *Systems and Transforms with Applications in Optics,* (McGraw-Hill, New York, 1968), pp. 43-44.

5. Ref. 4, p. 147.

6. H. H. Barrett and F. A. Horrigan, Appl. Opt. 12, 2686 (1973).

7. H. H. Barrett and G. D. DeMeester, Appl. Opt. 13, 1100 (1974).

MATHEMATICAL OPTICS

Design Modules and Optical Calculations
(O. N. Stavroudis)

These two research areas consist of developing new concepts and their realization in the form of computer programs in the area of modular optical design. In addition, general-purpose time-sharing computer programs are being developed for optical analysis and optical design.

Optical Design Modules

In the past quarterly report we described how modules became concentric at a particular value of the shape parameter. This value of the shape parameter is now included in our list of critical values calculated in our module programs. Concentric modules can be used to form concentric lenses. Such lenses have the useful properties of any concentric lens -- zero coma and astigmatism; zero distortion and lateral color. In addition, third-order spherical aberration is zero. However, Petzval and therefore field curvature tend to be large. For the camera lens configuration axial color can be made equal to zero in the manner described in earlier reports. However, Petzval cannot. The equation for zero Petzval, in this instance, turns out to be insoluable.

The reason for this is that a pair of hard-way coupled concentric modules will have a zero Petzval sum. Because a camera lens must contain an odd number of modules, the entire Petzval contribution must reside in the final module. The matrix of coefficients of the zero-Petzval equation becomes singular.

In the modular design of a copy lens the first and last modules are "odd" modules in this sense because all the others are hard-way

couples and therefore contribute nothing to the Petzval sum. It would appear to be possible to have the Petzval contribution of the two extreme modules cancel out exactly resulting in a concentric copy lens with no field curvature. It turns out, however, that this can work only for unit magnification and even then the image distance becomes virtual. This feature certainly disqualifies the design as a copy lens; it might be useful as a loupe -- although even in that case there is no particular advantage in having a zero field curvature.

In the concentric form of the module all pupils coincide with the common center of curvature. One can ask if it is not possible for a similar event to occur for some particular parameter value. A module consists of two spherical refracting surfaces. Suppose that an aplanatic point of the first surface coincides with an aplanatic point of the second. Then the remaining two aplanatic points would be conjugates of one another. If the two module pupils coincided with these, then we would have a module configuration distinct from the concentric case but with many of its advantages and with the possibility that one could build up a lens system for which Petzval could be satisfied. It turns out, unfortunately, that this configuration is inconsistent with the basic property of a module -- that it be free of spherical aberration.

This does suggest that it may be possible to define an entirely different kind of module, one for which third-order spherical aberration is not corrected but that contains the aplanatic configuration as a special shape parameter value. This might be important in broadening the number of building blocks available for use in modular optical design.

In addition to adding the "concentric point" to the list of critical values to be calculated in our computer programs a number of other more important changes have been made. In previous reports we have described how, "in principle" distortion and lateral color could be made zero simultaneously before the other aberrations were corrected. However, because the two equations were highly nonlinear the task was

by no means an easy one. In most cases we could correct one or the other of these aberrations, but not both together. During the past quarter we have developed an iterative procedure, dubbed RELAX appropriately enough, which does exactly this. Working on the shape parameters of the last two modules it finds values for which distortion and lateral color are zero.

This is shown in Fig. 8, a print-out from program CAM2 that generates camera designs from, in this case, five modules. This lens is nominally a 40 in. $f/10$ camera lens with a semi-field angle of 20°. The top five lines (A) give the case, parameter value, and category of each of the five modules. Next (B) come the coefficients of the power parameters in the equations for zero coma, zero Petzval, and zero axial color. The equations for distortion and lateral color do not depend on the power parameters and can be calculated once and for all at this stage. The values appear at (C).

With five modules any pair of these three aberrations may be made zero simultaneously. Here we choose coma and Petzval. The five values of the power parameters are printed at (D) and the corresponding optical design, at (E), obtained from the power parameters and the canonical optical parameters calculated elsewhere in the program. The program stores these data in the sequential file ZCØPE1 designated at (F).

Because the equation for zero coma is a quadratic we can expect two distinct solutions. A second is seen at (G). However, the computer determines that the design corresponding to this set of power parameters has a negative thickness in the first module, and the design is suppressed.

Note that this program automatically finds the stop location. Wherever a pupil is real (rather than virtual) and in air, the program will print out its location.

Figure 9 shows the printout of first and third-order calculations from program THRAYA. I believe it is self-explanatory. Note that under "sums of aberrations" at the bottom of the page only axial color is not equal to zero.

```
                                    DISTORTION    LAT COLOR
    1   REAL.    0.11700000   A2    6.7871E-02   -3.9978E-03
    2   REAL   -0.09040000    D1    3.172BE-01   -1.0621E-02
(A) 3   REAL   -0.10865000    D1    2.8935E-01   -6.7806E-03
    4   REAL   -0.16195660    A2    1.0464E-02   -5.1728E-04
    5   REAL    0.10636721    A1    1.5746E-03   -3.5975E-04
            COMA         PETZVAL.      AX COLOR       DISTOR       LAT COLOR
    1   -5.0269E-01    2.6624E-0.   -9.5623E-03   -5.2733E-01    6.6230E-03
(B) 2    1.6988E-01   -5.1114E-01    7.4705E-03    5.2459E-01   -6.2633E-03
    3    5.9802E-02    8.9047E-01   -1.4536E-02    2.7438E-03   -3.5975E-04
                                                  -8.8711E-07   -1.3315E-09  (C)

    F1 = 47.98
    F2 =-35.0302
    F3 =-30.5833
(D) F4 = 31.7337
    F5 = 30.302'
      T = -2.0480135E+01    AIR
    SPHERE C =   3.7089864E-02
      T =  3.4716519E+00   N =  1.80802   DEL N =  0.019841
    SPHERE C =   6.9798539E-02
      T =  1.8618670E+00   N =  1.67003   DEL N =  0.014222
    SPHERE C =  -3.99227140E-02
      T =  1.3019502E+01   N =  1.60311   DEL N =  0.009952
    SPHERE C =   5.29103816E-02
      T =  2.6952509E+00    AIR
    STOP            1.5289484 4E+00
    SPHERE C =  -1.00704290E-01
      T =  2.1894923E-01   N =  1.46450   DEL N =  0.007063
    SPHERE C =   6.8A308856E-02
(E)   T =  2.2756362E+00   N =  1.66882   DEL N =  0.011655
    SPHERE C =  -1.93531112E-01
      T =  1.3502366E-01    AIR
    SPHERE C =  -2.14564672E-01
      T =  4.4326467E-01   N =  1.46450   DEL N =  0.007063
    SPHERE C =  -1.86310174E-01
      T =  3.7378899E+00   N =  1.95250   DEL N =  0.046774
    SPHERE C =  -1.10811986E-01
      T =  3.5576942E+01    AIR
    TYPE IN FILE NAME
(F) ?ZCOPE1
    F1 =-26.5552
    F2 = 19.3879
    F3 =-15.8307
(G) F4 = 16.4263
    F5 = 30.3026
    NEGATIVE THICKNESS IN MODULE  1
```

Fig. 8. Printout from program CAM2.

```
              MARGINAL      PRINCIPAL
PUPIL   Y = 2.0000F+00   0.0000F+00
SPHFRF  Y = 2.0000F+00   7.4542F+00   SPH = 1.3792F-04 COMA =-1.63F0F-04
        I = 7.4058F-02  -R.7950F-02 ASTG = 1.9452F-04 PFTZ =-1.6549F-02
        U = 3.3097F-02   3.2466F-01 CURV = 6.2177F-03 DIST =-7.3F41F-03
                                     AX'L =-1.6254F-03 LTRL = 1.9303F-03
SPHFRF  Y = 1.8R51F+00   6.3270F+00   SPH =-1.3792F-04 COMA =-1.6379F-04
        I = 9.R4ROF-02   1.1695F-01 ASTG =-1.9452F-04 PFTZ = 3.1P9RF-03
        U = 2.4960F-02   3.1500F-01 CURV =-1.3555F-03 DIST =-1.609RF-03
                                     AX'L = R.2498F-04 LTRL = 9.7974F-04
SPHFRF  Y = 1.8386F+00   5.7405F+00   SPH = 1.0R55F-04 COMA = 6.0052F-04
        I =-9.R363F-02  -5.441RF-01 ASTG = 3.3223F-03 PFTZ =-9.9790F-04
        U = 2.9066F-02   3.3772F-01 CURV = 3.6R55F-03 DIST = 2.03R9F-02
                                     AX'L =-6.9711F-04 LTRL =-3.R567F-03
SPHFRF  Y = 1.4602F+00   1.3436F+00   SPH =-1.0R55F-04 COMA = 6.0052F-04
        I = 4.R194F-02  -2.6662F-01 ASTG =-3.3223F-03 PFTZ = 1.9906F-02
        U = 4.6566F-10   4.9852F-01 CURV =-1.0567F-02 DIST = 5.R462F-02
                                     AX'L = 7.0035F-04 LTRL =-3.R746F-03
STOP    Y = 1.4602F+00  -1.9372F-07
SPHFRF  Y = 1.4602F+00  -7.6221F-01   SPH =-6.906RF-04 COMA =-1.9R10F-03
        I =-1.4705F-01  -4.2176F-01 ASTG = 5.6R19F-03 PFTZ =-3.19A1F-02
        U =-4.6640F-02   3.6475F-01 CURV =-1.7307F-03 DIST =-4.96A1F-02
                                     AX'L = 1.0356F-03 LTRL = 2.9702F-03
SPHFRF  Y = 1.4704F+00  -8.4207F-01   SPH = 6.906RF-04 COMA =-1.9R10F-03
        I = 1.4726F-01  -4.2237F-01 ASTG = 5.6R19F-03 PFTZ =-5.7209F-03
        U =-2.8610F-02   3.1304F-01 CURV = 7.7641F-03 DIST =-2.2649F-02
                                     AX'L =-6.R534F-04 LTRL = 1.9657F-03
SPHFRF  Y = 1.5355F+00  -1.5544F+00   SPH = 3.5623F-02 COMA = 1.6190F-03
        I =-2.6856F-01  -1.2206F-02 ASTG = 7.3581F-05 PFTZ =-7.7562F-02
        U = 1.5101F-01   3.2120F-01 CURV = 2.8304F-02 DIST = 2.2R66F-03
                                     AX'L =-4.R063F-03 LTRL =-2.1R45F-04
SPHFRF  Y = 1.5151F+00  -1.597RF+00   SPH =-3.5623F-02 COMA = 1.6190F-03
        I =-4.7611F-01   2.1636F-02 ASTG =-7.3582F-05 PFTZ = 6.R055F-02

        U = 0.0000F+00   3.2806F-01 CURV =-2.4R44F-02 DIST = 1.1291F-02
                                     AX'L = 3.4790F-03 LTRL =-1.5R11F-04


SPHFRF  Y = 1.5151F+00  -1.7432F+00   SPH =-6.4268F-03 COMA =-7.475F-05

        I =-2.822RF-01  -3.2R33F-03 ASTG =-8.6943F-07 PFTZ = 3.1794F-02
        U =-7.0553F-02   3.2724F-01 CURV =-1.1574F-02 DIST =-1.30A1F-04
                                     AX'L = 1.19R4F-02 LTRL = 1.3939F-04


SPHFRF  Y = 1.77RRF+00  -2.9664F+00   SPH = 6.4268F-03 COMA =-7.4752F-05
        I =-1.2656F-01   1.4721F-03 ASTG = 3.6947F-07 PFTZ =-5.40555F-02
        U = 5.0000F-02   3.25R4F-01 CURV = 1.9676F-02 DIST =-2.2R66F-04
                                     AX'L =-1.0531F-02 LTRL = 1.2249F-04
IMAGF   Y = 2.2352F-07  -1.4559F+01       SUMS OF ABERRATIONS
                                     SPH =-1.1642F-10 COMA = 1.14235F-09
                                     ASTG =-1.591RF-09 PFTZ = 2.7942F-09
                                     CURV =-3.026RF-09 DIST = 1.2169F-07
                                     AX'L =-3.2066F-04 LTRL = 3.2560F-10
```

Fig. 9. Printout of first- and third-order
         calculations from program THRAYA.

Time-Sharing Computer Program

At the present time we are working on only one addition to our repertoire, program HEPTA for calculating third-order image and pupil aberration coefficients, fifth-order aberration coefficients, and seventh-order spherical aberration coefficient. In addition, it will calculate primary and secondary chromatic aberration coefficients.

Diffraction Theory
(A. S. Marathay)

A theoretical basis was formulated to study the diffraction of
light from apertures whose amplitude transmittance is specified on a
portion of a sphere. The theory calculates the diffraction pattern over
the surface of an observation sphere concentric with the aperture sphere.
This is analogus to conventional diffraction theory where the aperture
is situated in a plane and the diffraction pattern is calculated over
a parallel plane at some distance. In this formulation an appropriate
Green's function is constructed by use of the eigenfunctions of the
Helmholtz equation for spherical geometry such that it vanishes on the
sphere. The diffracted amplitude is expressed as an integral on the
surface of the sphere that involves only the amplitude distribution in
the aperture. In terms of the Laplace coefficients the integral re-
duces to a product relation that allows us to define the transfer
function of free space. The normal derivative of the Green's function
plays the role of the impulse response of the diffraction problem. We
are going to devise appropriate computer programs to allow us to cal-
culate typical diffraction patterns in this theory and compare them
with the conventional diffraction patterns.[1]

In the Fourier space formulation of diffraction theory for aper-
tures in a plane it is necessary to use Weyl's formula. This formula
gives the Fourier transform of the space part of an expanding spherical
wave. The derivation of Weyl's formula is much involved. We were
able to show that it may be derived as a natural consequence of the
inhomogenous Helmholtz equation satisfied by the Green's function of
the problem. This simpler derivation gives more insight into the
diffraction problem and is also pedagogically advantageous.

Radiometry

The fundamental laws of (noncoherent) radiometry have never
been derived from the basic (wave) theory of light. Several attempts
have been made in the literature, notably by Walther[2] and Marchand and
Wolf,[3] to derive these laws. Their formulations are unsatisfactory
for several reasons: (1) they introduce certain mathematical functions
without any physically measurable properties--they are merely mathe-
matical constructs, and (2) their results indicate that for a nonco-
herent source the radiant intensity behaves as $\cos^2\theta$ where θ is the
angle that the detector makes with the normal to the surface. That is,
they show that a noncoherent source is not Lambertian. This state of
affairs is unacceptable.

We therefore felt it was necessary to reformulate the theory to
generalize the laws of radiometry to partially coherent fields, such
that it will reproduce the well-known laws of radiometry. We present
a new approach to generalizing the laws of radiometry to partially
coherent fields. A new complex cross-correlation function F is in-
troduced that depends on two space points, two directions, and the
time difference τ. This function, F, and the mutual coherence function,
Γ, are the basis for defining the generalized radiometric quantities.
Special forms of the generalized radiance L are studied. These defini-
tions are applied to two special cases. In particular we show that a
uniform, noncoherent source of infinite extent is Lambertian. In partic-
ular for this source our generalized functions reduce to the traditional
radiometric quantities and we also successfully rederive their inter-
relationships. The relationships are[4]

$$\Phi_0 = \mathcal{A} M_0$$
$$M_0 = \pi L_0$$

and

$$I_0 = \mathcal{A} L_0 \cos\theta,$$

where Φ is the flux with units of W, M_0 is the radiant emittance
W m^{-2}, I_0 is the radiant intensity W sr^{-1}, and the radiance L_0 has the
units of W m^{-2} sr^{-1}. The quantity $\mathcal{A}$ is the area element of the source.

References

1. A. S. Marathay, to be published in J. Opt. Soc. Am., June 1975.
2. A. Walther, J. Opt. Soc. Am. 58, 1256 (1968).
3. E. W. Marchand and E. Wolf, J. Opt. Soc. Am. 64, 1219 (1974).
4. A. S. Marathay, to be published.

Image Plane Speckle

(M. J. Lahart and A. S. Marathay)

We have finished the main theoretical aspect of our work concerning reduction of speckle by using weak diffusers. Our calculations have been based on the study of second-order statistics. In particular, we calculated the intensity correlation function of the speckle pattern as a function of the aperture size of the imaging system and of the characteristics of the diffuser.

Diffusers are used in coherent optical systems to reduce diffraction noise from dust or blemishes. They cause the dust particle or noise source to be illuminated from several directions so that the effects of noise are spread out or averaged and generally made less apparent. The process of averaging can create speckle or some other artifact, however, and designers of coherent systems must know how to control both speckle and diffraction noise and reduce their combined effect.

We have investigated the way diffraction noise is reduced by a diffuser by computing its effect on several individual noise patterns produced by small particles. Noise of this kind is nearly eliminated if light is scattered through a relatively small minimum angle, and it is reduced only little more if light is scattered through much larger angles. The contrast of the speckle pattern may be high if light is scattered through larger angles than necessary, however, unless the aperture size is also large. The minimum scattering angle is an important design parameter because it determines how large the system aperture must be to restrict speckle contrast to an acceptable level.

Recently it has been recognized that random phase plates can be used to scatter light through small angles. The speckle pattern that is produced is the spatially filtered image of the phase object, and its contrast is small if nearly all of the light is transmitted by the

system. Phase plate diffusers can permit light to be scattered through the minimum angle necessary to reduce diffraction noise, without scattering it through the larger angles that make speckle more apparent.

A random phase plate scatters light through large angles like a strong, ground glass diffuser if the phase variance is large and the phase correlation distance is small. Light may be scattered through smaller angles if the phase correlation length is large, but the scattering distribution may be coarse and uneven, especially if the correlation length is comparable to the dimensions of the diffuser. If the phase correlation distance is small, the phase variance must also be small. However, if the variance is too small, the specular component of the radiation, the light that is transmitted without being scattered, may be large, so that the effectiveness of the diffuser is reduced. A phase plate that is used as a noise reducing diffuser should have a small specular component, but a small enough phase variance so that the correlation distance can be small.

Our work has shown that if the phase of a random diffuser is normally distributed, the percentage of specularly transmitted light is small when the phase standard deviation is one or two radians. Not only is almost all of the light scattered in this case, but the detailed characteristics of the scattering distribution can be specified because the distribution is nearly proportional to the phase Wiener spectrum. These small phase standard deviations appear to be the optimum for noise reducing diffusers in imaging systems.

We have investigated the image speckle pattern of weak diffusers in detail. The speckle contrast can be surprisingly high even when most of the diffracted light is transmitted, but it sometimes consists primarily of high spatial frequencies. (This is not true of speckle patterns of strong diffusers.) The optical system can sometimes be designed to eliminate speckle noise that is not in the same part of the spatial frequency spectrum as the image; the speckle may not be objectionable when this is the case.

The statistical law that the phase obeys was found to have an important influence on the speckle pattern. Diffusers whose phase was negative exponentially distributed created higher contrast patterns and scattered less light than those whose phase was normally distributed. We found that techniques for making negative exponential diffusers can be modified to produce normally distributed diffusers with prescribed phase Wiener spectra.

We investigated the influence of the coherence of the illumination on the speckle pattern. The speckle contrast is small if the light coherence length is sufficiently short, but moderately incoherent light can produce a speckle pattern whose Wiener spectrum is dominated by low spatial frequencies but whose contrast is nearly the same as a coherent light pattern. Partially coherent illumination is often proposed as a solution to the speckle problem; our work shows that its use is not always a good solution, and it can even make the problem worse.

Some work was necessary to delineate the regions of validity of our computations because most of our calculations are ensemble averages. The ergodic theorem guarantees that a single pattern can be characterized by its ensemble average if it is large enough, but this characterization may not be appropriate if the pattern is of finite size. We analyzed the statistical accuracy of finite pattern calculations and showed that ensemble averages are accurate under many but net all practical conditions, and we established minimum sizes of formats under which they are good descriptors.

OPTICAL TRACKING

(J. C. Wyant)

Optical Tracking System

The optical tracking system study for the Space and Missile Test Center (SAMTEC) at Vandenberg Air Force Base has continued to fulfill the seven technical tasks described in the past SAMSO quarterly report. An interim report was written giving the progress to date. The report describes recent work in optical detection systems that establishes the limits of accuracy and performance capability of state-of-the-art optical tracking systems for collecting metric data on the Western Test Range. While imaging systems cannot provide the desired metric data, they can aid in the tracking of a laser radar system and can also give engineering data. As long as the missile is equipped with a retro-reflector, a laser ranger can give the missile range to within a 10-cm error, and a laser Doppler system can give the missile velocity to within an error of 0.01 ft/sec or less during the burn stages of the missile any time of the day or night, as long as the sun is not directly within the field of view and the weather is clear.

Use of White-Light Extended Source with a Lateral Shear Interferometer for Real-Time Wavefront Correction Systems

An analysis was performed to determine the accuracy with which an ac heterodyne lateral shear interferometer can measure wavefront aberrations if a white-light extended source is used with the interferometer and shot noise is the predominant noise source. The analysis shows that for uniform circular or square sources larger than a derived minimum size, the wavefront measurement accuracy depends on only the radiance

of the source and not on the angular subtense of the source. For a
radiance of 10 W/m^2 sr the rms wavefront error is approximately 1/30 wave,
assuming the singal is shot noise limited. For both uniform circular
and square sources an optimum shear distance is approximately half the
aperture diameter required to resolve the light source. The analysis is
of particular importance because of the use of lateral shear interferom-
eters in active optics systems, especially for systems in which wavefront
deformations introduced by atmospheric turbulence are being corrected.

Etched Gratings

Work is continuing on the fabrication of etched gratings in glass.
The techniques are believed useful for active optics systems in which
changes in the figure of the primary mirror are being measured. Because
the gratings are etched in the mirror surface directly, there is no
problem in the grating moving relative to the mirror surface. Because
the etch depth is small and the diffraction orders are out of the field
of view, the etched grating will not affect the performance of the optical
system. Progress during the past quarter includes improving the repeat-
ability of the grating-forming process and improving the uniformity
of a 2-in.-square grating. Work is presently being performed to make a
6-in.-diam grating on a parabolic mirror.

Comparison of Heterodyne and Direct Detection Systems

An analysis is being performed to compare the signal-to-noise
ratios of heterodyne and direct detection systems in the presence of
atmospheric turbulence and several background radiation levels. The
particular wavelength of interest is 10.6 µm, although the use of shorter
wavelengths is also being investigated.

QUANTUM OPTICS

Picosecond Spectroscopy
(J. C. Matter, M. O. Scully, A. L. Smirl)

The measurement of the intraband lifetime of carriers in semi-
conductors has shifted from germanium[1] to mercury cadmium telluride,
$Hg_{1-x}Cd_xTe$. This material was chosen chiefly for two reasons:
(1) HgCdTe is a direct band gap semiconductor[2] in contrast to indirect
gap germanium, which may provide a simpler model for theoretical analysis;
and (2) the width of the band gap can be selected by varying the alloy
parameter x,[3] the mole fraction of cadmium telluride (CdTe).

We do not have definitive experimental results to present at
this time. It has become apparent that surface preparation, i.e.,
etching, is an important factor for HgCdTe, while for germanium it is
not (for these experiments). This seems reasonable in light of the
fact that HgCdTe is a much softer solid than Ge. Thus, when the sample
is being polished, surface damage may be much more severe for HgCdTe
than for Ge.

We will briefly describe the experiments performed thus far.
For unetched samples of HgCdTe, no saturation of transmission at high
intensities (λ = 1.06 μm) was observed and subsequently no lifetime was
measured. For HgCdTe samples etched on the front (incident radiation)
surface, saturation of transmission was observed for one sample of large
x value. Lifetime curves were obtained as a function of temperature
and as a function of excitation pulse intensity. In order to determine
if this observed lifetime is dominated by the unetched back (mounted
on KZF-2 glass substrate) surface, we are now preparing new samples
that will be etched on both surfaces.

References

1. SAMSO 75-112, Semi-annual FY75 Applied Optics Research Report, Jan. 1975.

2. D. J. Chadi and M. L. Cohen, Phys. Rev. B7, 692 (1973).

3. J. L. Schmit and E. L. Stelzer, J. Appl. Phys. 40, 4865 (1969).

Transient Interactions
(R. L. Shoemaker and E. Van Stryland)

During the past quarter we have successfully made direct
measurements of transition dipole matrix elements in a molecule using
optical nutation. The transition dipole matrix element, $\mu_{ab} = \int \psi_a^* \, e\vec{r}\psi_b d\tau$,
is an important parameter in any spectroscopic experiment since it is
$|\mu_{ab}|^2$ that fundamentally determines the strength of a transition from
the state ψ_a to the state ψ_b. Accurate values of μ_{ab} are useful in a
wide variety of applications including the study of population dis-
tributions in gases, radiative energy transfer problems, and the search
for new laser transitions. In addition, for vibrational transitions in
molecules, the vibrational piece of μ_{ab} can be used as a test for vi-
brational potentials and wave functions. Thus accurate methods for
measuring transition dipole matrix elements are of considerable interest.

We have demonstrated how direct, accurate measurements of tran-
sition dipole matrix elements can be made using optical nutation. This
phenomenon is seen as a damped oscillation in the transmitted intensity
that occurs when a molecular transition is suddenly brought into re-
sonance with a laser beam. The oscillation arises because molecules are
driven coherently back and forth between the ground and excited states
producing an alternating absorption and emission of radiation. If the
transition is excited exactly on resonance by a uniform optical field
with amplitude E_0, the oscillation frequency is just $\mu_{ab}E_0/\hbar$. Thus a
measurement of the oscillation frequency together with a measurement of
the laser intensity $I = \frac{1}{2}c\varepsilon_0 E_0^2$ gives the matrix element μ_{ab} directly.

Transition dipole matrix elements can also be determined from
curve of growth measurements where the absolute absorption as a function
of pressure is measured. This method can give accurate results, but
only when certain conditions are met. Optical nutation is complementary
to the curve of growth method in the sense that the accuracy of the two

techniques depends on different parameters so that one can often be used in situations where the other fails.

Our optical nutation measurements were made on the deuterated ammonia, NH_2D, using a Stark switching technique described below. Transition dipole matrix elements are obtained for two vibration-rotation transitions in the molecule, and since the transition assignments are known, the vibrational piece of the transition dipole matrix elements along two different axes in the molecule can be determined. These quantities should provide a sensitive test of the ν_2 vibrational wave function. in NH_2D.

There has been one previous attempt to measure a transition dipole matrix element using optical nutation. Hocker and Tang made a measurement on SF_6 using a pulsed laser. It is hard to assess the accuracy of their results because of the difficulties inherent in a pulsed laser experiment. In particular, the nutation frequency varies because the optical field strength changes during the pulse and the laser frequency can be chirped. It is also difficult to measure accurately the nutation signal that does occur, since it appears as a small signal on a time varying background. Furthermore, a determination of the optical field strength is extremely difficult since the pulse shape, the pulse energy, and the transverse profile of the beam must all be reproducible and accurately known. Thus the measurement of transition dipole matrix elements using this approach does not appear very promising if accuracies much beyond an order of magnitude estimate are desired.

The difficulties just mentioned can be avoided, however, by using the Stark switching technique developed by Brewer and Shoemaker. In this method, which we have used for the measurements reported here, a cw laser is utilized and molecular transitions are shifted in and out of resonance using the Stark effect. Thus, one merely passes the laser beam through the sample and applies a pulsed electric field across it. The optical nutation signal is observed by monitoring the transmitted light with a photodetector. Using a pulsed electric field instead of a pulsed laser produces several significant advantages. First, because the laser beam

is cw, it produces only a dc signal in the detector. The only ac signal present is just the optical nutation signal one wants to observe! This allows the nutation signal to be accurately measured. Second, since the pulsed electric field can be a nearly ideal step function and the cw laser is stable in amplitude and frequency, an exact theoretical calculation of the optical nutation signal can be made with μ_{ab} as the only adjustable parameter. Finally, the laser intensity may be accurately measured by using a calibrated thermopile to obtain the total beam power and a scanning aperture to obtain the beam's transverse intensity profile. Thus one expects that accurate measurements of μ_{ab} can be made, and we have found that these expectations are fulfilled.

A fundamental limitation of the Stark switching technique is, of course, that transitions with a substantial Stark effect must be used. However, the technique can be generalized by frequency switching the laser instead of the sample. Optical nutation can then be observed in any transition that overlaps a laser line.

We have developed a semiclassical treatment of optical nutation that can be quantitatively compared with our experiments. We wish to consider what happens when a cw laser beam passes through a low pressure gas sample with a resonant, nondegenerate transition. The laser frequency ω_L is assumed initially to be somewhere within the Doppler broadened linewidth of the transition (~ 80 MHz FWHM for NH_2D at $\lambda = 10$ μm). Only these molecules with a z component of velocity $v_z{}'$, such that they are Doppler shifted into resonance, are excited, and this narrow velocity group has a homogeneous linewidth that is typically 100 kHz to 1 MHz FWHM. At $t = 0$, a step function electric field is applied across the sample that shifts the center frequency of the transition to a new value. If the frequency shift is several homogeneous linewidths or more, a new velocity group, $v_z{}''$, will suddenly be shifted into resonance producing an optical nutation signal. In addition to the optical nutation, there will also be an optical free induction decay signal (FID) from the velocity group, $v_z{}'$, that was shifted out of resonance. This signal can be ignored in practice because the FID appears as a heterodyne beat with the laser and decays

as $\exp[-\gamma t - \sqrt{\gamma^2 + (\mu_{ab}E_0/\hbar)^2}t]$, where γ is the collisional decay rate.
Thus the FID has essentially died out by the end of the first cycle of
optical nutation, and even during that cycle, its amplitude can be made
negligibly small by simply Stark shifting far enough to make the heter-
odyne beat frequency lie outside the bandwidth of the detection system.
In light of this we may neglect the previously excited velocity group,
v_z', and consider only the response of an unexcited transition suddenly
shifted into resonance at $t = 0$. Our approach is to calculate the molec-
ular polarization by means of the density matrix equations of motion,
and then to use Maxwell's equation to find the signal that appears at
the detector.

We take the optical field to be

$$E_L = E_0 \cos(\Omega_L t - kz). \tag{1}$$

Considering now an ensemble of molecules with axial velocities between
v_2 and $v_z + dv_z$, and making a (nonrelativistic) transformation to a
moving coordinate frame in which these molecules are at rest, this
becomes

$$E_L = E_0 \cos(\Omega_L't - kz'), \tag{2}$$

where $\Omega_L' = \Omega_L - kv_z$ and z' is the molecular position in the moving
frame. We assume an optically thin sample so that E_0 does not depend
on z. This condition is certainly satisfied in our experiments where the
peak absorption is ~0.3%.

The equation of motion for the molecular density matrix can be
written

$$\dot{\vec{\rho}} = -\frac{i}{\hbar}[\vec{\mathcal{H}},\vec{\rho}] -\frac{1}{\tau}(\vec{\rho} - \vec{\rho}^0), \tag{3}$$

where $\vec{\rho}^0$ is the density matrix in thermal equilibrium and we have intro-
duced a single phenomenological decay time τ. This is equivalent to the
assumption that the molecular relaxation processes are dominated by
strong collisions in which the collisional transition probability to any

level is simply proportional to the Boltzmann factor for that level. Such an assumption is not in fact justified for the NH$_2$D transitions studied here since the relaxation time for the population difference, $\rho_{bb} - \rho_{aa}$, and the relaxation time for the off-diagonal element ρ_{ab} differ. However, for low sample pressures the decay of the observed optical nutation signal is dominated by effects due to the transverse intensity profile of the laser beam. Thus the collisional decay model one uses does not significantly affect the results of the calculation, and we can proceed using the simple strong collision model.

Upon solving Eq. (3), calculating the resulting polarization, and using Maxwell's equations to find the transmitted intensity, we obtain

$$I(t) = I_0 - \frac{\mu_{ab}^2 E_0^2 \Omega_L L (N_b - N_a)}{4\hbar\Delta\omega_D\sqrt{\pi}} \int_{-\infty}^{\infty} k \, \exp\left[\frac{-(kv_z)^2}{(\Delta\omega_D)^2}\right]\left\{\frac{1}{g}e^{\frac{-t}{\tau}} \sin 2gt \right.$$

$$\left. - \frac{2\tau}{1 + 4g^2\tau^2}\left[1 - e^{\frac{-t}{\tau}}\left(\cos 2gt + \frac{1}{2gt} \sin 2gt\right)\right]\right\}dv_z, \quad (4)$$

where $I_0 = c\epsilon_0 E_0^2/2$ and $g = \frac{1}{2}[(kv_z)^2 + (\mu_{ab}E_0/\hbar)^2]^{\frac{1}{2}}$. In the limit as $t \to \infty$, this equation reduces to the standard expression for steady-state saturated absorption at the peak of a Doppler broadened line. For short times $\exp(-t/\tau) \to 1$, and the integral in Eq. (4) can be evaluated approximately to give $2\pi J_0[(\mu_{ab}E_0/\hbar)t]$. Since the zero order Bessel function J_0 is approximately unity for small t, the initial peak value of the optical nutation signal will be

$$\Delta I_{peak} = \frac{\mu_{ab}^2 E_0^2 \Omega_L (N_b - N_a) L\sqrt{\pi}}{2\hbar\Delta\omega_D} . \quad (5)$$

We note that Eq. (5) is exactly the expression one obtains for *unsaturated* absorption assuming a small optical field. This is not unexpected since for a short time after the molecules are switched into resonance, the level populations have not yet changed appreciably and one sees the full unsaturated absorption.

Experiment

A block diagram of the experimental arrangement is shown in
Fig. 10. A 1.5 m grating-controlled CO_2 laser is used that produces
approximately 2 to 4 W, TEM_{00} mode, on any one of approximately 50 CO_2
lines. A small 650 Hz dither is applied to the output mirror producing
a variation in the discharge tube impedance. This signal is used to
lock the laser to the peak of its gain curve with a long-term frequency
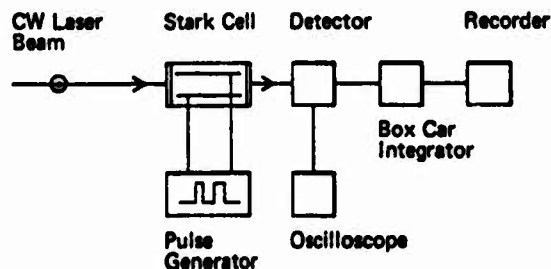stability of ±1 MHz. The short-term frequency jitter is less than 100 KHz.

CW Laser   Stark Cell   Detector   Recorder
Beam

Box Car
Integrator

Pulse   Oscilloscope
Generator

Fig. 10. Block diagram of the experimental arrangement.

The NH_2D gas samples are held in a Stark cell equipped with
NaCl windows and containing two 4 x 30 cm long glass plates metallized
on their inner surfaces and separated by .5946 ± .0005 mm quartz spacers.
After passing between the Stark plates, the transmitted laser beam is
monitored by Au:Ge photoconductive detector, that in combination with a
preamplifier, has a bandwidth of approximately 10 MHz. A pulse generator
supplies step function voltage pulses across the Stark plates at a
repetition rate of approximately 20 kHz, and the detector-preamp output is
fed into a PAR 162 Boxcar integrator that provides signal averaging
and displays the results on an x-y recorder.

NH$_2$D was synthesized by simply mixing NH$_3$ and D$_2$O. The H and D atoms in both NH$_3$ and D$_2$O exchange rapidly among themselves, resulting in a statistical mixture of partially deuterated water and ammonia. This mixture was vacuum distilled several times holding the mixture at -78°C and collecting the distillate at -196°C. Since the vapor pressure of H$_2$O is 10^{-3} Torr at -78°C, as compared to 50 Torr for NH$_3$, all water can be removed in this manner. The purified ammonia mixture contains 45% NH$_2$D if the NH$_3$:D$_2$O ratio is 1.33:1 by volume.

We first examined the $(\nu, J, M_J) = (1, 4_{04}, 4) \rightarrow (2, 5_{14}, 5)$ NH$_2$D transition that was Stark tuned approximately 2300 MHz into resonance with the $P(14)$ CO$_2$ laser line at 949.48 cm^{-1}. The Stark field is perpendicular to the optical field direction such that $\Delta M_J = \pm 1$ selection rules apply, the $\Delta M_J = \pm 1$ transition being by far the more intense. This could readily be made more accurate in future experiments. We also measured μ_{ab} using a lower laser power, 1.28 W at 3.9 mTorr. Here the signal is correspondingly more sensitive to τ because the nutation frequency is lower. However, the fit is still good (see Fig. 11) and yielded a value of $\mu_{ab} = .0356 \pm .0021$ Debye. This differs from the higher power measurement by only 2%. The average value for the dipole moment is $\mu_{ab} = .0353 \pm .0021$ Debye. We also made measurements on two M components of the $(\nu, J) = (0, 4_{04}) \rightarrow (1, 5_{05})$ transition that may be Stark tuned into resonance with the $P(20)$ CO$_2$ laser line at 949.19 cm^{-1}. This transition involves a three-level system arising from a small Stark and quadrupole splitting of the upper level. This splitting causes a quantum beat in the nutation signal. As discussed in a previous report, we have calculated the expected nutation signal in this three-level system and found the possible deviation in the value of μ_{ab} from the two-level theory to be less than 15%. The deviation should be small since one of the upper states has a much smaller dipole matrix element connecting it to the lower level. The values obtained for μ_{ab} are

$$\mu_{ab} = .0355 \quad \text{for} \quad M_J = 4 \rightarrow 5, \text{ and}$$

$$\mu_{ab} = .0295 \quad \text{for} \quad M_J = 3 \rightarrow 4.$$

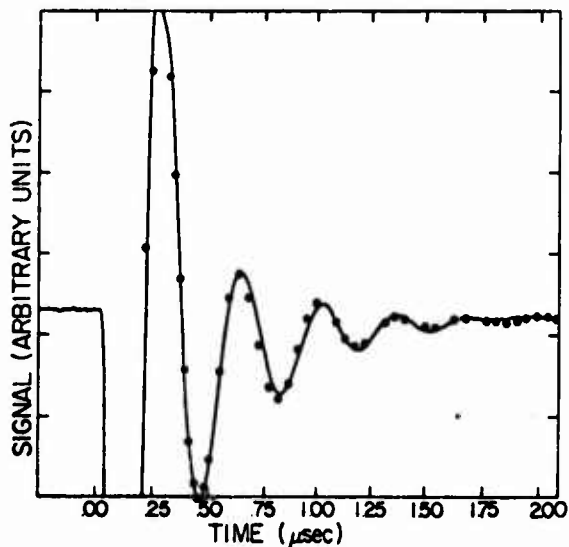Taking into account the M_J value degeneracy factors these values agree to within 7%.

Fig. 11. Experimental nutation signal using 3.9 mTorr of
NH$_2$D and a laser output power of 1.28 W.

From these values for the total dipole moments, the vibrational piece is extracted as follows: the upper and lower state wave functions are expanded in terms of the symmetric rotor basis wave functions, and μ_ν is obtained from

$$\mu_\nu = \frac{\mu_{total}}{\langle \psi_{lower} | \phi | \psi_{upper} \rangle},$$

where the denominator is just the rotational direction cosine matrix element.

This transition involves a single nondegenerate two-level system so that the above-described theory applies. The experimental nutation signal using 6.6 mTorr of NH_2D and a laser output power of 2.34 W is shown in Fig. 12 along with the theoretical fit. Note that the detector sees the field emitted by all the molecules interacting with the laser beam because of diffraction at 10.6 µm. We verified this by varying the aperture directly behind the cell and noted that the nutation signal remained unaltered. Therefore, since the laser field E_0 is a function of R, the radial distance from the center of the beam, the signal S must be the integral of Eq. (4) over R

$$S = 2\pi \int_0^\infty I(t)R \, dR. \tag{6}$$

where $I(t)$ is now a function of R. The beam profile, $E_0^2(R)$, was very nearly Gaussian and was obtained by measuring the laser power both in front of and behind the Stark cell using a small scanning aperture in the vertical and horizontal directions. These profiles were averaged, and Eq. (6) was numerically integrated to obtain the curve of Fig. 12.
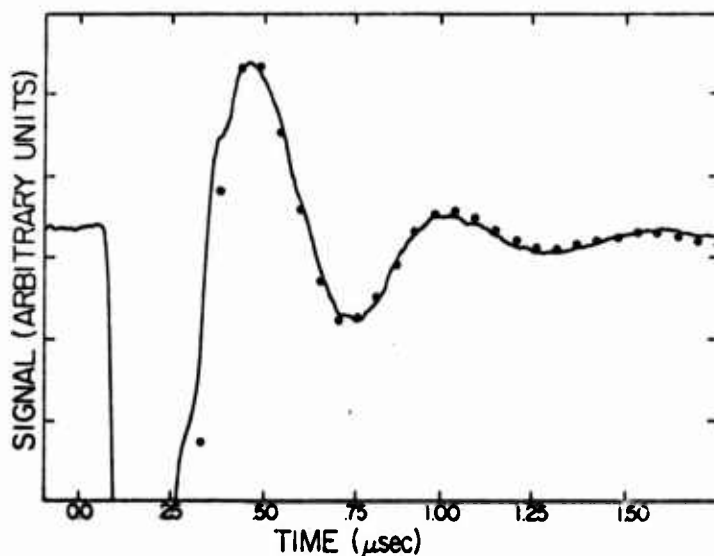

Fig. 12.   Experimental nutation signal using 6.6 mTorr of NH D and a laser output power of 2.34 W.

The value of τ, the lifetime, and $\mu_{ab}E_0/\hbar$, where E_0 is now the peak field intensity, are $\tau \simeq 1.2$ μsec and $\mu_{ab}E_0/\hbar = 9.0 \pm .5$ MHz. The errors are set by a 2% fitting error and a 5% beam area measurement error. The fit was very insensitive to the value chosen for τ. This is due to the fact that the nutation signal from the molecules in the center of the beam (high power and thus high frequency) and the edge of the beam (low power and low frequency) interfere to give a short lifetime for the nutation signal. From the value of $\mu_{ab}E_0/\hbar$ the dipole moment can be determined if we know E_0. E_0 is given by the absolute power measurement. This power was measured with a Coherent Radiation model 210 power meter that had been calibrated to within 5% with a CO_2 laser against a standard traceable to the National Bureau of Standards. We used the average of two such meters that checked to within 4%.

The value of the dipole moment that resulted is $\mu_{ab} = .0349 \pm .002$ Debye. The bulk of the error here is due to the beam profile measurement.

The value of μ_ν obtained for the $P(14)$ transition was $.156 \pm .014$ Debye, whereas for the $P(20)$ transition, $\mu_\nu = .097 \pm .015$. These results are the vibrational transition dipole matrix elements along the c and a principal axes in the molecule, respectively. To our knowledge, these results represent the first measurements of vibrational dipole matrix elements ever made in an asymmetric rotor molecule.

## Electromagnetic Anisotropy
(J. Small)

An experimental test for anisotropy in the velocity of light has been designed after the method of E. W. Silvertooth.[1] The experiment consists of propagating highly stabilized electromagnetic frequencies between two points. The entire experiment is then rotated to detect differential changes in propagation velocity with respect to direction. A detailed analysis shows that the absolute frequencies used are unimportant, but the fractional frequency stability of the oscillators contributes directly to the signal-to-noise ratio of the experiment.

Frequency stability is a precisely defined mathematical concept[2] that depends upon the sample time during a frequency measurement. Differences between short-term and long-term stability are thus rigorously quantified. In the present test, the sample times of interest are determined by the rotation rate of the experimental apparatus. It is highly important that the oscillators used have adequate frequency stability during a single rotation period.

The oscillators chosen for the experiment are methane-stabilized helium-neon lasers operating at a wavelength of 3.39 μm. They have excellent stability. "The frequency stability from 1 msec out to ten seconds matches or exceeds the stability of other oscillators which have been used as standard frequency sources, e.g., hydrogen masers, cesium beam devices, crystal oscillators, etc."[3] In addition, the short infrared wavelength eliminates many experimental difficulties, such as multipath propagation and diffraction effects, that would be encountered with microwave or radio frequency oscillators.

The flow diagram of Fig. 13 shows the construction plan for the experimental apparatus. Progress to date is indicated by heavy underlining. The work divides naturally into three general areas: (1) con-

Fig. 13. Construction plan for the experimental apparatus.
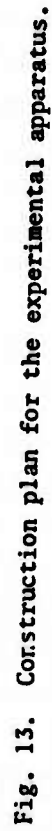
struction of the stable lasers, (2) construction of an air-cushioned rotating table, and (3) computer-controlled data analysis.

The laser frequency stabilizing electronics are being constructed under the supervision of the National Bureau of Standards in Boulder, Colorado. When integrated with the ULE quartz laser cavities presently under construction at the Optical Sciences Center, frequency stabilities equal to the present state of the art may be expected.

References

1. E. W. Silvertooth, to be published.
2. See, for example, H. Hellwig, "Frequency standards and clocks: a tutorial introduction," National Bureau of Standards Technical Note 616 (revised), March 1974.
3. H. Hellwig, A. E. Bell, P. Kartaschoff, and J. C. Bergquist, "Frequency stability of methane-stabilized He-Ne lasers," J. Appl. Phys. 43, 450 (1972).

Atomic and Molecular Physics Laboratory
(W. Wing)

Work has continued on establishing the Atomic and Molecular Physics Laboratory in the Physics Department. The equipment for three experiments brought from Yale University in the summer of 1974 is being set up, and reassembly of one experiment (on infrared resonance in molecular ions) is finished. A dye laser pumped by a nitrogen laser is being constructed to excite Rydberg states in helium atoms. A new experiment has begun on the pumping mechanism of the helium-neon laser.

One copy to each addressee unless otherwise indicated.

HQ USAF (AFRDSA)
Washington, D.C. 20330

HQ USAF (AFRDSD)
Washington, D.C. 20330

Secretary of the Air Force (SAFRD)
Washington, D.C. 20330

HQ AFSC (DLSS)
Andrews AFB
Washington, D.C. 20331

HQ USAF (AFRDR)
Washington, D.C. 20330

Capt Edward Dietz   (9 copies)
SAMSO/DYS
PO Box 92960
Worldway Postal Center
Los Angeles, California   90009

Defense Documentation Center (DDC)   (12 copies)
Cameron Station
Alexandria, Virginia 22314

Air University Library
Maxwell AFB, Alabama 36112

Air Force Avionics Laboratory
Wright-Patterson AFB, Ohio 45433   (2 copies, 1 copy to AVRO)

Air Force Cambridge Research Laboratory (CRO)
L.G. Hanscom Field
Bedford, Massachusetts 01730

Aeronautical Systems Division (ASRS)
Wright-Patterson AFB, Ohio 45433

Air Force Office of Scientific Research (SRPP)
1400 Wilson Blvd.
Arlington, Virginia 22209

Air Force Weapons Laboratory (LRO)
Kirtland AFB, New Mexico 87117

David Smith   (3 copies)
Itek Corporation
Lexington, Massachusetts 02173

Rod Scott   (3 copies)
Perkin Elmer Corporation
50 Danbury Road
Norwalk, Connecticut 06851

Sarah Hise
SAMSO/DYK
PO Box 92960
Worldway Postal Center
Los Angeles, California 90009